JCTC Journal of Chemical Theory and Computation

Derivation of Distributed Models of Atomic Polarizability for Molecular Simulations

Ignacio Soteras,[†] Carles Curutchet,[†] Axel Bidon-Chanal,[†] François Dehez,[‡] János G. Ángyán,*[,§] Modesto Orozco,*[,∥,⊥] Christophe Chipot,*[,‡] and F. Javier Luque*[,†]

Departament de Fisicoquímica and Institut de Biomedicina, Facultat de Farmàcia, Universitat de Barcelona, Avgda, Diagonal 643, Barcelona 08028, Spain, Équipe de Dynamique des Assemblages Membranaires, Unité Mixte de Recherche CNRS/UHP 7565 and Équipe Modélisation Quantique et Cristallographique, LCM3B UMR 7036, Nancy Université, BP 239, 54506 Vandoeuvre-lès-Nancy Cedex, France, Departament de Bioquímica i Biología Molecular, Facultat de Química, Universitat de Barcelona, c/. Martí i Franqués 1, 08028, Barcelona, and Unitat de Modelització Molecular i Bioinformàtica, Institut de Recerca Biomèdica, Parc Científic de Barcelona, c/. Josep Samitier 1, 08028 Barcelona, Spain

Received May 14, 2007

Abstract: The main thrust of this investigation is the development of models of distributed atomic polarizabilities for the treatment of induction effects in molecular mechanics simulations. The models are obtained within the framework of the induced dipole theory by fitting the induction energies computed via a fast but accurate MP2/Sadlej-adjusted perturbational approach in a grid of points surrounding the molecule. Particular care is paid in the examination of the atomic quantities obtained from models of implicitly and explicitly interacting polarizabilities. Appropriateness and accuracy of the distributed models are assessed by comparing the molecular polarizabilities recovered from the models and those obtained experimentally and from MP2/Sadlej calculations. The behavior of the models is further explored by computing the polarization energy for aromatic compounds in the context of cation-π interactions and for selected neutral compounds in a TIP3P aqueous environment. The present results suggest that the computational strategy described here constitutes a very effective tool for the development of distributed models of atomic polarizabilities and can be used in the generation of new polarizable force fields.

Introduction

The assumption that induction effects can be treated in an average sense by means of an appropriate parametrization justifies the success of pairwise, additive potential energy functions for cost-effective statistical simulations of organic and biomolecular systems. An important ingredient in the development of such force fields consists in increasing artificially the polarity of the participating molecules to mimic intermolecular induction phenomena.[1] A popular approach for implicit polarization is based upon the observation that, compared to the experimental gas-phase quantities, molecular dipole moments computed at the Hartree−Fock (HF) level with a split-valence 6-31G(d) basis set are systematically exaggerated.[2] Thus, it has thus become customary to use net atomic charges derived by fitting the HF/6-31G(d) electrostatic potential or suitably scaled HF/

* Corresponding author e-mail: fjluque@ub.edu (F.J.L.), Christophe.Chipot@edam.uhp-nancy.fr (C.C.), modesto@mmb.pcb.ub.es (M.O.), Janos.Angyan@lcm3b.uhp-nancy.fr (J.G.A.).
[†] Facultat de Farmàcia, Universitat de Barcelona.
[‡] Unité Mixte de Recherche CNRS/UHP 7565, Nancy Université.
[§] LCM3B UMR 7036, Nancy Université.
[∥] Facultat de Química, Universitat de Barcelona.
[⊥] Institut de Recerca Biomèdica.

10.1021/ct7001122 CCC: $37.00
Published on Web 09/29/2007

6-31G(d) interaction energies in the development of nonpolarizable force fields.[3−11]

The effective polarization implicit to two-body force fields is not equivalent to a rigorous, atomic-level description of the molecular response to a nonuniform, external electric field. This has been illustrated by numerous studies that have examined structural[12−24] and energetic[25−28] properties on a variety of chemical and biochemical systems. The growing body of evidence that induction forces can play a pivotal role in the fine description of the structural and energetic features of highly polarizable systems, in conjunction with the enhanced computational capabilities witnessed in recent years, has stimulated the development of strategies to treat polarization explicitly in classical simulations. Much effort has, therefore, been invested to explore the suitability of such induction schemes such as fluctuating charge[29−33] or induced point dipole[34−45] models, Drude oscillators,[46−48] modified sets of atomic charges,[49−51] or schemes that combine the above.[52−54]

The implementation of explicit polarization schemes is associated with the availability of models of distributed atomic polarizabilities, which are neither uniquely defined nor physically measurable. The partitioning scheme put forward by Stone,[55,56] which merges an earlier formulation of the susceptibility function of the charge density[57] with the distributed multipole analysis method,[58] provides distributed polarizabilities from quantum mechanical (QM) calculations of the response of an isolated molecule to an external perturbation. A closely related procedure[59] relies on a topological partitioning of the molecular space into atomic regions, according to the *atoms-in-molecules* (AIM) theory.[60] These models yield polarizabilities that reproduce the induced moments due to a local electrostatic potential and its successive derivatives experienced at another site. Nevertheless, they include a plethora of terms that rapidly become cumbersome to handle, thus limiting their usefulness in force field simulations.

Applequist derived a heuristic approach wherein atomic polarizabilities were derived by minimizing the deviation between calculated and experimental molecular polarizabilities.[34] This strategy, which was originally devised in the framework of the induced dipole model, was subsequently refined through the introduction of a modified polarizability tensor to smear out the dipole interaction[61] or by extending the model to monopole and dipole polarizabilities.[62] Alternative schemes rely upon atomic hybrid, bond, or group polarizabilities[63] or have resorted to the fitting of molecular polarizabilities determined from QM calculations with large basis sets.[64,65] An inherent feature of these approaches is a substantial component of arbitrariness in the parametrization of the model and the assumption of transferability of the atomic polarizabilities.

In the spirit of the electrostatic potential-fitted (ESP) charge approach,[66−68] alternative schemes targeted at the construction of models of distributed polarizabilities based on a least-squares fitting to the induction energy have been devised.[69−72] Their strength resides in the possibility of generating rather easily compact, flexible sets of polarizability parameters at any given order. Their main limitation stems from the enormous cost associated with the computation of induction energies, since in its most straightforward formulation it requires N_p distinct QM calculations to evaluate the induction energy due to the presence of a nonpolarizable point charge placed at any of the N_p points used to discretize the space around the molecule. This shortcoming has been recently circumvented in two computational strategies that rely essentially upon a single QM calculation. The first scheme is based on second-order perturbation theory (PT) and, upon suitably chosen scaling factors, reproduces the variational induction energy from one QM calculation at the HF level.[73−75] The second strategy consists of mapping grids of induction energies from a single high-level QM calculation, followed by a topological partitioning of the electron density (TPED) response into atomic regions.[59,76] For neutral molecules, induction energies obtained from PT and TPED schemes agree closely.[75]

In the present study, the PT strategy is used to derive distributed models of atomic polarizabilities in the framework of the induced dipole theory for a set of neutral molecules which includes prototypical organic compounds. The atomic polarizabilities are derived by considering their implicit and explicit interaction. The quality of the models is assessed in a comparison of the molecular polarizabilities recovered from the models with both experimental and MP2/Sadlej values. In addition, the ability of the atomic polarizabilities to reflect the induction energy determined for selected chemical interactions (i.e., cation-π complexes and neutral polar solutes in aqueous solution) is examined. The results are discussed in the light of the potential implementation of the distributed models in classical force fields.

Methods

Induction Energies. The variational calculation of the induction energy (U_{ind}) due to a nonpolarizable point charge (q_k) placed at point $\mathbf{r}_k$ in the space surrounding a molecule is expressed as

$$U_{ind} = E_{total,k} - E^\circ - q_k V(\mathbf{r}_k) \tag{1}$$

where $E_{total,k}$ is the total energy of the molecule in the presence of the point charge at $\mathbf{r}_k$, E° is the energy of the isolated molecule, and $V(\mathbf{r}_k)$ is the electrostatic potential created by the isolated molecule at $\mathbf{r}_k$.

Within the PT approach, the induction energy appears at the second order of perturbation energy and is given by

$$U_{ind} = \left\langle \psi^{(o)} \middle| \frac{q_k}{|\mathbf{r}_k - \mathbf{r}|} \middle| \psi^{(1)} \right\rangle \tag{2}$$

where $\psi^{(o)}$ and $\psi^{(1)}$ denote the wave function of the isolated molecule and its first-order correction term, respectively.

In the framework of the Hartree−Fock (HF) theory, eq 2 can be approximated as[73]

$$U_{ind} = \sum_{a}^{occ} \sum_{r}^{vir} \frac{1}{\epsilon_a - \epsilon_r} \left[\sum_{\mu} \sum_{\nu} c^*_{\mu a} c_{\nu r} \left\langle \varphi_\mu \middle| \frac{q_k}{|r_k - r|} \middle| \varphi_\nu \right\rangle \right]^2 \tag{3}$$

where ϵ_a and ϵ_r stand for the energy of occupied and virtual molecular orbitals, respectively, and ϕ_μ and ϕ_ν correspond to atomic orbitals in the occupied and virtual molecular orbitals.

The strength of the PT scheme embodied in by eq 3 lies in its reduced computational cost, as only one single QM calculation at the HF level is required to estimate the density matrix. The induction energies, however, tend to be underestimated in absolute value relative to the variational ones, as expected from the fact that eq 3 is based upon an uncoupled form of the HF equations. Such a deviation can, nevertheless, be corrected by an appropriate scaling of the PT induction energies.[75,78] In particular, we have used here the distance-dependent scaling factor defined by eq 4,[75] which was derived by comparing the exact (MP2/Sadlej) and PT induction energies for a series of small neutral compounds

$$\zeta(r) = \frac{\alpha_{\text{exact}}}{\alpha_{\text{UCHF}}}\left(a_o + \frac{a_1}{r} + \frac{a_2}{r^2}\right) \tag{4}$$

where α_{exact} and α_{UCHF} are the exact (i.e., the derivative of the energy with respect to the electric field) and the uncoupled HF estimates of the molecular polarizability, and a_x ($x = 0, 1, 2$) are adjustable parameters.

Atomic Polarizabilities. For all intents and purposes, the distributed models of atomic polarizabilities have been derived in the framework of the induced dipole theory, though an extension to other models is straightforward. For the sake of simplicity, in all cases off-diagonal components of the polarizability tensor of the constituent atoms have been neglected in all cases. The atomic dipole components have been imposed to be isotropic.

Two different procedures have been considered to account for the coupling between distributed units.[79] In the model of explicitly interacting distributed polarizabilities, the many-body nature of the polarizability response experienced by the molecule due to the presence of the nonpolarizable point charge (q_k; see above) is accounted for by an explicit interaction between the different units, which in the induced dipole model is summarized in

$$U_{\text{ind}} = -\frac{1}{2}\sum_i \mu_i E_i^\circ \tag{5}$$

where μ_i is the induced dipole created at atom i, and E_i° is the local external electric field applied to the molecule.

The induced dipole (see eq 6) depends on the point atomic dipole polarizabilities, α_i°, and the total local electric field, E_i, which consists of the permanent electric field and that generated other induced dipoles (eq 7)

$$\mu_i = \alpha_i^\circ E_i \tag{6}$$

$$E_i = E_i^\circ - \sum_{j\neq i} T_{ij}\mu_j \tag{7}$$

where T_{ij} is the ijth element of the dipole field tensor.

Equations 5−7 are solved iteratively during the fitting to the PT induction energies until self-consistency in the induced dipoles is achieved. The induction energy is then determined as

$$U_{\text{ind}} = -\frac{1}{2}\sum_i \alpha_i^\circ E_i E_i^\circ \tag{8}$$

In the model of implicitly interacting distributed polarizabilities, the coupling of the polarizability response of the different subunits is omitted during the fitting to the PT induction energies, so that the induction energy is expressed as

$$U_{\text{ind}} = -\frac{1}{2}\sum_i \alpha_i^{\text{eff}} E^\circ E_{ii}^\circ \tag{9}$$

Equation 9 simplifies the calculation of the induction energies, while assuming that the fitting of atomic polarizabilities is able to capture the coupling between the induced dipoles located at the different polarizable sites of the molecule. It is, therefore, worth stressing that the atomic polarizabilities appearing in eqs 8 and 9 are different, as the many-body nature of the induction energy is taken into account explicitly (α_i°) during the derivation of the distributed models used in eq 8. In contrast, these effects are assumed to be incorporated implicitly into the effective atomic polarizabilites (α_i^{eff}) used in eq 9.

Computational Details. The PT induction energies of eq 3 were determined for a variety of neutral compounds, which include small molecules (CH_4, CO, H_2O, H_2S, HF, CO_2, NH_3), organic compounds containing prototypical functional groups (C_2H_6, C_2H_4, C_2H_2, C_6H_6, CH_3OH, CH_3NH_2, CH_3F, CH_3CN, CH_3OCH_3, $HCOCH_3$, CH_3COCH_3, HCOOH, CH_3CONH_2, $CH_3CH_2NO_2$, CH_3COOCH_3), heterocyclic rings (pyridine, pyrrole, furan, imidazole, and indol), and a series of aromatic derivatives (fluorobenzene, chlorobenzene, phenol, aniline, benzonitrile, 1,4-difluorobenzene, and 1,3,5-trifluorobenzene).

The computation of the molecular polarizabilities, the value of which largely depends on the level of theory,[80−84] was performed at the MP2 level using the Sadlej basis set.[83] This protocol has proven to offer a good compromise between accuracy and computational investment.[75] The geometry optimizations were performed at the MP2/6-31G-(d,p) level, and the molecular polarizabilities were estimated subsequently at the MP2/Sadlej level using the Gaussian03 suite of programs.[84]

The grids of PT induction energies were determined from the HF/Sadlej wave function using the MOPETE[85] program. The grids were constructed by using the OPEP program[86,87] and fixing the multiplicative factor (ξ) for the atomic van der Waals radii[88] of atoms to 5. The number of points (N_p) was adjusted by varying the grid step (see ref 86 for details). Using this procedure, the dependence of the polarizability models on the density of points was examined by varying N_p from ca. 500 to ca. 5000 points.

The isotropic atomic polarizabilities used in eqs 8 and 9 (models A and B, respectively) were restrained to be positive during the fitting procedure in order to avoid physically unrealistic values due to the excessive simplicity of the model. Moreover, in the model of explicitly interaction polarizabilities (eq 8; model A), the coupling between induced dipoles borne by contiguous atoms (1−2 and 1−3

interactions) was neglected, since their interaction is assumed to be described appropriately by the bonded terms implemented in classical force fields. In addition, Thole's damping function[61] was used whenever necessary to couple the induced dipoles located at non-neighboring (1−4 interactions or greater) sites. Following Thole's approach, the scaling distance used to smear out the dipole interaction was built up from the atomic polarizabilities of the interacting sites. The fitting of the PT induction energies was performed using the FITPOL program.[89] Finally, the effect of eliminating the restraint that forces atomic polarizabilities to be positive was investigated for the model of implicitly interacting polarizabilities (eq 9; model C). In this case, the fitting was performed using the OPEP program.

Results and Discussion

Effect of the Grid. Based on a previous series of experiments on the influence of the grid on QM electrostatic potential derived atomic point charges, the definition of the grid over which the induction energies are mapped can be a critical factor on the models of distributed atomic polarizabilities. Contrary to the grids used to fit point charges, it has been noted that mapping of induction energies must sample regions of space far enough from the nuclei to warrant an appropriate reproduction of molecular polarizabilities.[75] Accordingly, grids have been constructed in such a way that only those points located between envelopes corresponding to 2 and 5 times the atomic van der Waals radii are considered. Here, our attention is focused mainly on the density of points defined between these envelopes.

The dependence on the grid density of the atomic and the molecular polarizabilities obtained for the three models is illustrated in Table 1 and Figure 1 for four representative molecules, viz. methanol, methylamine, acetone, and acetamide. The results clearly demonstrate that both atomic and molecular polarizabilities remain only marginally affected by the density of points, except for those grids involving less than ca. 1000 points. From a practical point of view, it can be concluded that for the set of small and medium sized molecules examined here models of atomic dipolar polarizabilities can be derived from grids containing ca. 1500 points, which corresponds to a grid step of about 1.3 Å. In the following the discussion will be limited to the results obtained using above definition of the grid.

Atomic Dipole Polarizabilities. Table 2 shows the atomic dipole polarizabilities obtained for models A−C for the whole set of neutral molecules considered in this investigation.

The analysis of the results shown in Table 2 reveals qualitative differential trends in the dipole polarizabilities between certain atom types. For instance, the larger polarizability of third-row atoms is reflected in the comparison of the values obtained for S (ca. 22 au^3) and Cl (ca. 21 au^3) relative to O (ca. 8 au^3) and F (ca. 5 au^3). Likewise, polar hydrogen atoms, i.e., bonded to N, O, and F, bear polarizabilities (ca. 1.7 au^3) lower than those found for hydrogen atoms in benzene (ca. 3.3 au^3). The polarizabilities of the nitrogen atom in methylamine and aniline are rather similar (ca. 12 au^3), just like for the nitrogen atom in acetonitrile and benzonitrile (ca. 15 au^3), the fluorine atom in methyl fluorine and fluorobenzene, 1,4-difluorobenzene, and 1,3,5-trifluorobenzene (ca. 6 au^3), and the oxygen atom in methanol and phenol (ca. 8 au^3), which in turn differs from the polarizability of the oxygen atom in those compounds featuring a carbonyl moiety (ca. 12 au^3). The different polarizability borne by the two nitrogen atoms in imidazole is also worth underlining, amounting to about 7 and 13 au^3 for NH and N, respectively, and hence resembling the values obtained for the nitrogen atom in pyrrole (ca. 6.5 au^3) and pyridine (ca. 14 au^3). Moreover, the polarizability of the carbon atom in benzene (ca. 8.5 au^3) lies close to the average value determined for the carbon atoms in the monosubstituted benzene derivatives (excluding the carbon atom bearing the substituent). Yet, the results also show that the atomic polarizabilities depend on the nature of the substituent and the position of the carbon atom relative to that substituent.

The preceding trends support the generally accepted assumption of a certain degree of transferability for the atomic polarizability of atom types in specific chemical groups. Great care must, however, be taken in the physical interpretation of the distributed models due to anomalous atomic polarizabilities generally found for occluded atoms, such as the carbon atom in methyl or carbonyl groups and the carbon atom bearing the substituent in benzene derivatives. In these cases model C generally yields negative atomic polarizabilities, which are shown to be close to zero in models A and B, where positivity restraints are enforced. This behavior stems mainly from the statistical fitting

Table 1. Dependence of Atomic Dipolar Polarizabilities (in au^3) Obtained from Models A−C on the Number of Points Used for Mapping of Induction Energies for Methanol, Methylamine, Acetone, and Acetamide[a]

	A (eq 8, $\alpha>0$)			B (eq 9, $\alpha>0$)			C (eq 9, no restraint)		
atom	500	1500	5000	500	1500	5000	500	1500	5000
				CH_3OH					
O	7.7	7.5	7.7	7.6	7.4	7.6	10.9	10.4	10.6
H(O)	1.7	1.8	1.7	1.8	1.9	1.8	2.3	2.3	2.1
C	0.1	0.1	0.1	0.1	0.1	0.1	−13.3	−10.6	−10.1
H(C)	3.7	3.8	3.8	3.7	3.8	3.8	7.2	6.6	6.5
				CH_3NH_2					
N	9.4	11.2	11.2	8.8	11.1	10.9	11.6	14.6	13.7
H(N)	2.1	1.6	1.6	2.3	1.6	1.7	2.7	2.0	2.0
C	0.1	0.1	0.1	0.1	0.1	0.1	−8.8	−10.5	−7.6
H(C)	3.9	3.8	3.8	4.0	3.8	3.8	6.4	6.6	6.0
				CH_3COCH_3					
O	11.1	10.9	10.6	11.3	11.3	11.1	13.5	13.3	13.2
C(O)	4.2	4.4	5.2	2.9	2.7	3.2	5.3	4.7	5.6
C	0.1	0.1	0.1	0.1	0.0	0.0	−7.9	−5.7	−6.5
H(C)	3.9	4.0	3.9	4.1	4.1	4.1	6.4	5.8	6.0
				CH_3CONH_2					
O	13.6	12.2	12.2	12.7	11.5	11.5	13.6	14.1	13.9
C(O)	0.1	0.1	0.1	1.0	0.9	0.1	0.9	−0.9	−1.0
N	10.9	8.3	8.6	11.9	9.2	9.6	11.8	10.9	12.8
H(N)	2.2	2.2	2.1	1.8	1.9	1.9	2.1	2.3	1.8
C	0.2	0.2	0.1	0.2	0.1	0.1	−9.2	−5.2	−5.5
H(C)	4.5	4.1	4.1	4.6	4.1	4.2	6.7	6.0	6.0

[a] Only values obtained for around 500, 1500, and 5000 points are shown.

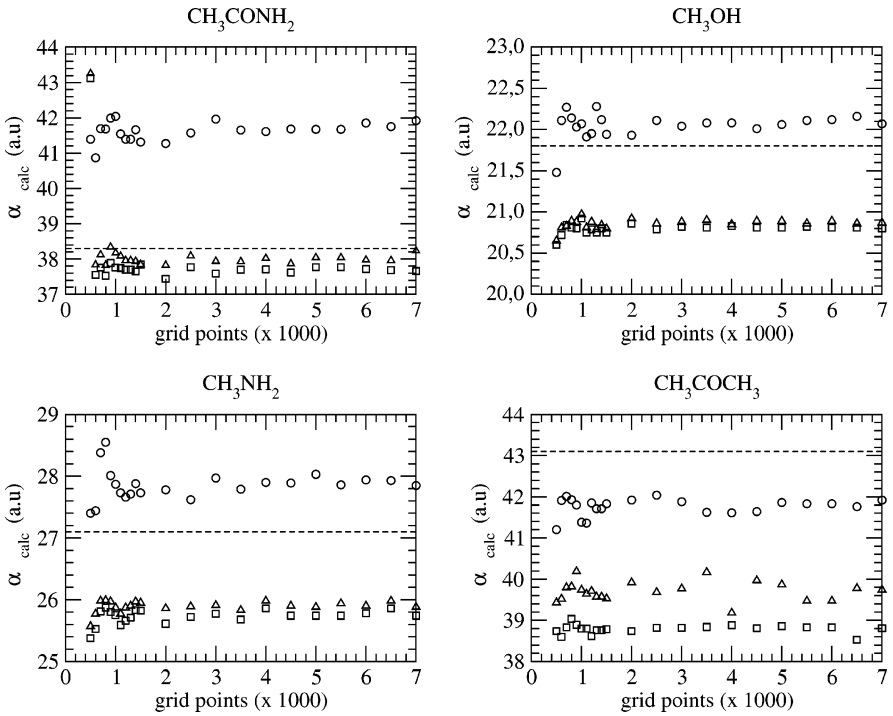

Figure 1. Dependence of the molecular polarizability (in au^3) derived from atomic polarizabilities obtained for models A (eq 8, $\alpha>0$; triangle), B (eq 9, $\alpha>0$; square), and C (eq 9, no restraint; circle) on the number of points used for mapping of induction energies for methanol, methylamine, acetone, and acetamide.

performed to minimize the difference between the reference and the calculated induction energies. Thus, even though the distributed models are mathematically consistent, their physical meaning can be affected by the anomalous values assigned to atoms buried in the interior of the molecule. To alleviate this effect, one possibility might consist in enforcing suitable restraints to the polarizabilities of those eclipsed atoms during the fitting procedure. Alternatively, it is reasonable to expect that more elaborate models of distributed polarizabilities, including for instance charge-flow and quadrupole polarizabilities, or where ill-defined components are eliminated,[71,72] should yield more realistic models.

Finally, it is also worth noting that upon exclusion of those compounds with less than four atoms or with negative atomic polarizabilities, there is in general a close similarity between the atomic polarizabilities derived for models A−C (see the Supporting Information), as noted by the scaling coefficient (c) of the regression equations α(model A) = c α(model B) (c = 1.05, r = 0.98, F = 675.8), α(model A) = c α(model C) (c = 0.92, r = 0.98, F = 885.7), and α(model B) = c α(model C) (c = 0.88, r = 0.99, F = 3530.0; in the preceding equations r is the Pearson's correlation coefficient, and F is the Snedeckor's distribution parameter). Within the specific conditions imposed here to the mathematical models used in eqs 8 and 9 (see Methods), the similar results obtained for distributed models of explicitly or implicitly interacting atomic polarizabilities mainly reflects the large screening effect introduced in model A by neglecting the coupling between induced dipoles borne by contiguous atoms (see above).

Molecular Polarizabilities. The reliability of the models of distributed atomic polarizabilities can be checked from their ability to reproduce the molecular polarizability. Table 3 reports the molecular polarizabilities determined from MP2/Sadlej computations and from experimental measurements[90] for the series of compounds and the corresponding values obtained from models A−C.

The root-mean-square deviation (rmsd) between the experimental and the calculated molecular polarizabilities is comparable in the three models, ranging from 2.2 to 3.3 au.[3] Yet, whereas model C tends to overestimate slightly the molecular polarizability with a mean deviation of 1.7 au,[3] the reverse trend is found for models A and B, which underestimate the molecular polarizability by 1.6 and 2.5 au,[3] respectively. Figure 2 shows the regression equations obtained for the comparison of the experimental and the calculated values. In all cases there is a close agreement between the calculated and the experimental polarizabilities, as noted in the scaling coefficients of equation α_M(exptal) = c α_M(model), which amount to 1.04 (r = 1.00, F = 10746), 1.06 (r = 1.00, F = 9635.2), 1.07 (r = 1.00, F = 8329), and 0.96 (r = 1.00, F = 4291) for models A−C, respectively.

Induction Energies. The suitability of the distributed models can be further checked by examining the induction energies for cation-π interactions, where polarization plays a critical contribution to the total stabilization energy of the complex (see for instance ref 74).

The induction energy profiles determined for the approach of a positively charged particle toward benzene were determined from MP2/Sadlej computations and using the three distributed models. The profiles were computed for three possible orientations of the approaching particle (see Figure 3): (i) along the middle of a C−C bond (x-direction), (ii) along the C−H bond (y-direction), and (iii) perpendicular

Table 2. Atomic Dipolar Polarizabilities (in au^3) Obtained from Models A−C for the Series of Neutral Compounds

atom	A (eq 8, $\alpha>0$)	B (eq 9, $\alpha>0$)	C (eq 9, no restraint)	atom	A (eq 8, $\alpha>0$)	B (eq 9, $\alpha>0$)	C (eq 9, no restraint)	atom	A (eq 8, $\alpha>0$)	B (eq 9, $\alpha>0$)	C (eq 9, no restraint)
						CH_4					
C	0.0		−8.0	H(C)	4.0		6.3	rmsd[a]	0.02		0.01
						NH_3					
N	9.6		10.9	H	1.9		2.3	rmsd	0.07		0.09
						H_2O					
O	7.4		8.5	H	1.6		1.8	rmsd	0.06		0.07
						HF					
F	4.9		5.1	H	1.2		1.8	rmsd	0.04		0.05
						H_2S					
S	20.9		23.6	H	2.4		2.8	rmsd	0.05		0.06
						CO					
C	8.1		9.0	O	5.7		6.6	rmsd	0.06		0.07
						CO_2					
C	0.0		−11.6	O	9.4		15.2	rmsd	0.20		0.04
						C_2H_6					
C	4.5	0.0	−3.2	H	3.2	4.4	5.9	rmsd	0.04	0.02	0.03
						C_2H_4					
C	9.0	9.4	10.6	H	2.3	2.1	2.4	rmsd	0.07	0.07	0.08
						C_2H_2					
C	6.9	6.8	7.7	H	4.1	4.2	4.7	rmsd	0.04	0.04	0.05
						C_6H_6					
C	8.9	7.5	8.6	H	2.3	3.2	3.5	rmsd	0.06	0.07	0.08
						CH_3OH					
C	0.1	0.1	−10.6	H(C)	3.8	3.8	6.6	rmsd	0.03	0.04	0.03
O	7.5	7.4	10.4	H(O)	1.8	1.9	2.3				
						CH_3NH_2					
C	0.1	0.1	−10.5	H(C)	3.8	3.8	6.6	rmsd	0.05	0.05	0.05
N	11.2	11.1	14.6	H(N)	1.6	1.6	2.0				
						CH_3F					
C	0.0		−11.1	H(C)	3.6		6.6	rmsd	0.03		0.01
F	5.8		8.3								
						CH_3CN					
C(N)	0.1	0.1	−1.7	N	14.4	14.5	17.5	rmsd	0.04	0.04	0.04
C(H)	0.1	0.1	−1.3	H	4.1	4.1	5.1				
						CH_3OCH_3					
C	0.1	0.1	−11.3	H	3.8	3.9	6.8	rmsd	0.06	0.04	0.02
O	9.8	8.6	15.0								
						$HCOCH_3$					
C(O)	0.1	0.1	−3.5	$C(CH_3)$	0.2	0.2	0.2	$H(CH_3)$	4.3	4.3	4.8
O	11.0	11.0	14.7	H(C═O)	4.3	4.3	5.7	rmsd	0.06	0.05	0.06
						CH_3COCH_3					
C(═O)	4.4	2.7	4.7	$C(CH_3)$	0.1	0.0	−5.7	rmsd	0.04	0.03	0.03
O	10.9	11.3	13.3	H	4.0	4.1	5.8				
						HCOOH					
C	0.1	0.2	−8.6	O(H)	8.2	8.5	11.6	H(O)	1.2	0.9	1.2
O(═C)	9.8	9.9	14.0	H(C)	3.4	3.3	6.3	rmsd	0.06	0.06	0.05
						CH_3CONH_2					
C(═O)	0.1	0.9	−0.9	N	8.3	9.2	10.9	H(N)	2.2	1.9	2.3
C(H)	0.2	0.1	−5.2	H(C)	4.1	4.1	6.0	rmsd	0.07	0.04	0.05
O	12.2	11.5	14.1								
						$CH_3CH_2NO_2$					
$C(CH_3)$	0.1	0.1	−12.2	O	9.2	9.3	16.3	$H(CH_2)$	1.8	1.7	2.1
$C(CH_2)$	11.1	10.7	19.5	$H(CH_3)$	3.2	3.2	6.6	rmsd	0.13	0.12	0.08
N	0.1	0.1	−19.8								

Table 2 (Continued)

atom	A (eq 8, $\alpha>0$)	B (eq 9, $\alpha>0$)	C (eq 9, no restraint)	atom	A (eq 8, $\alpha>0$)	B (eq 9, $\alpha>0$)	C (eq 9, no restraint)	atom	A (eq 8, $\alpha>0$)	B (eq 9, $\alpha>0$)	C (eq 9, no restraint)
					CH_3COOCH_3						
C(−COO)	0.1	0.1	−6.6	O(=C)	11.9	11.3	13.3	H(CH_3O)	2.9	3.3	5.8
C(=O)	0.5	0.6	1.0	O(−CH_3)	11.9	9.0	14.0	rmsd	0.04	0.03	0.03
C(−OCO)	0.2	0.2	−10.0	H(CH_3C)	3.7	4.0	5.9				
					Pyridine						
C_α	0.1	0.1	−3.3	N	13.9	13.6	17.4	H(C_γ)	3.6	4.0	4.7
C_β	14.8	13.6	19.1	H(C_α)	4.0	4.5	5.4	rmsd	0.06	0.07	0.08
C_γ	0.1	0.1	−2.4	H(C_β)	2.3	2.6	2.2				
					Pyrrole						
C_α	5.5	5.9	6.7	H(C_α)	3.5	3.8	4.1	H(N)	1.9	2.5	2.8
C_β	11.3	10.4	11.8	H(C_β)	1.8	2.2	2.4	rmsd	0.06	0.06	0.08
N	7.7	5.7	6.5								
					Furan						
C_α	3.6	4.5	4.2	O	8.1	7.1	8.7	H(C_β)	2.0	2.4	2.4
C_β	10.2	9.2	11.0	H(C_α)	3.7	3.8	4.3	rmsd	0.05	0.06	0.07
					Imidazole						
C_2	0.1	0.1	0.1	N_3	13.4	13.5	15.2	H(C_5)	2.6	3.1	3.3
C_4	4.7	4.5	5.3	H(C_2)	4.4	4.6	5.1	H(N_1)	2.0	2.4	2.9
C_5	9.5	8.6	10.2	H(C_4)	3.0	3.3	3.6	rmsd	0.06	0.06	0.07
N_1	7.5	6.5	6.9								
					Indole						
C_2	0.1	0.1	−2.7	C_8	0.1	0.0	−13.7	H(C_4)	3.4	4.6	3.4
C_3	22.0	22.8	29.1	C_9	0.1	0.1	−4.2	H(C_5)	2.7	3.2	3.0
C_4	9.3	5.8	13.5	N	17.0	16.4	24.6	H(C_6)	1.8	2.3	2.3
C_5	8.7	7.9	10.2	H(N)	0.4	0.5	0.5	H(C_7)	3.7	3.8	3.9
C_6	12.6	14.3	14.7	H(C_2)	3.2	3.4	4.8	rmsd	0.07	0.09	0.09
C_7	8.0	6.0	12.4	H(C_3)	0.1	0.1	−0.6				
					Fluorobenzene						
C(F)	1.4	1.1	1.4	C_{para}	8.7	7.5	9.2	H(C_{meta})	2.2	3.2	3.3
C_{ortho}	10.8	9.5	10.3	F	5.7	6.0	6.7	H(C_{para})	2.5	3.2	3.1
C_{meta}	8.6	7.2	8.5	H(C_{ortho})	2.1	3.1	3.6	rmsd	0.06	0.06	0.08
					Chlorobenzene						
C(Cl)	0.1	0.1	−4.7	C_{para}	9.0	8.6	9.6	H(C_{meta})	2.2	3.4	3.3
C_{ortho}	12.1	8.8	12.6	Cl	18.5	19.4	22.7	H(C_{para})	2.6	2.9	3.2
C_{meta}	8.3	7.3	8.5	H(C_{ortho})	1.9	3.3	3.2	rmsd	0.05	0.06	0.07
					Phenol						
C(OH)	0.1	0.1	−1.3	O	7.5	7.8	9.2	H(C_{meta}/C'_{meta})	2.8/2.3	3.5/2.5	4.0/3.2
C_{ortho}/C'_{ortho}	12.2/12.3	9.9/10.1	12.2/12.9	H(O)	1.5	1.7	1.6	H(C_{para})	3.0	3.6	3.4
C_{meta}/C'_{meta}	6.7/7.3	6.9/9.2	6.1/7.9	H(C_{ortho}/C'_{ortho})	2.3/2.7	3.3/3.2	3.6/3.6	rmsd	0.06	0.07	0.08
C_{para}	9.7	7.3	10.9								
					Aniline						
C(NH_2)	0.1	0.1	−2.4	N	12.0	11.1	13.4	H(C_{meta})	2.8	3.5	3.7
C_{ortho}	13.2	10.1	13.1	H(N)	0.9	1.5	1.5	H(C_{para})	1.7	2.3	2.9
C_{meta}	4.6	5.4	6.1	H(C_{ortho})	2.4	3.5	3.6	rmsd	0.07	0.07	0.09
C_{para}	15.5	13.5	14.2								
					Benzonitrile						
C(≡N)	0.1	0.1	−4.5	C_{para}	8.1	8.8	10.6	H(C_{meta})	2.5	3.3	3.7
C(CN)	11.1	8.5	15.5	N	13.8	15.0	17.9	H(C_{para})	2.4	3.2	3.1
C_{ortho}	7.9	6.7	6.3	H(C_{ortho})	2.7	3.4	4.2	rmsd	0.07	0.08	0.09
C_{meta}	8.9	7.5	8.0								
					1,4−Difluorobenzene						
C(F)	0.2	0.1	−0.3	F	5.8	6.1	6.7	rmsd	0.05	0.06	0.07
C	11.8	9.8	11.5	H	1.6	2.9	3.1				
					1,3,5−Trifluorobenzene						
C(F)	0.1	0.1	-4.5	F	5.7	6.1	7.1	rmsd	0.05	0.06	0.07
C	13.8	12.4	18.8	H	1.9	2.5	2.2				

[a] Root-mean square deviation (in kcal/mol) between PT induction energies and the values recovered by the distributed models.

Table 3. Molecular Polarizabilities (in au^3) Determined from Atomic Dipolar Polarizabilities Obtained from Models A−C and MP2/Sadlej Computations and Measured Experimentally

molecule	A (eq 8, $\alpha>0$)	B (eq 9, $\alpha>0$)	C (eq 9, no restraint)	MP2/ Sadlej	exptl
CH_4	16.1	16.1	17.1	16.5	17.5
CO	13.8	13.8	15.6	13.3	13.2
H_2O	10.6	10.6	12.2	9.8	9.8
H_2S	25.7	25.7	29.1	24.6	25.5
HF	6.1	6.1	6.9	5.7	5.4
CO_2	18.8	18.8	18.8	18.6	19.6
NH_3	15.5	15.5	17.7	14.4	15.3
C_2H_6	28.2	26.4	28.7	28.3	30.2
C_2H_4	27.3	27.4	30.9	27.3	28.7
C_2H_2	21.9	21.9	24.8	22.8	22.5
C_6H_6	67.3	64.6	72.6	69.4	69.6
CH_3OH	20.8	20.8	21.9	21.1	21.8
CH_3NH_2	26.0	25.8	27.7	25.7	27.1
CH_3F	16.5	16.5	17.0	16.8	20.0
CH_3CN	27.2	26.9	29.9	30.2	30.2
CH_3OCH_3	32.8	32.3	33.0	33.4	34.8
$HCOCH_3$	28.6	28.3	31.4	30.2	31.0
CH_3COCH_3	39.5	38.8	41.9	41.9	43.1
HCOOH	22.7	22.7	24.5	22.9	22.9
CH_3CONH_2	37.9	37.9	41.3	39.8	38.3
$CH_3CH_2NO_2$	43.1	42.4	44.0	44.5	47.2
CH_3COOCH_3	44.8	43.3	46.7	46.1	46.0
pyridine	60.2	59.2	66.5	64.1	61.9
pyrrole	53.8	52.7	59.4	55.0	53.6
furan	47.0	46.6	52.5	48.6	48.8
imidazole	47.3	46.6	52.5	49.3	48.5
indole	94.5	91.3	101.2	102.8	NA
fluorobenzene	66.4	63.8	71.8	69.4	69.5
chlorobenzene	79.7	76.6	85.9	84.0	83.0
phenol	71.0	68.9	77.2	75.1	74.9
aniline	77.8	75.0	84.1	81.4	81.6
benzonitrile	80.4	77.4	86.8	86.4	84.3
1,4−difluorobenzene	65.9	63.2	71.0	69.3	66.1
1,3,5−trifluorobenzene	64.9	63.2	70.7	69.8	65.7
msd[a]	−1.6	−2.5	1.7	−0.1	
rmsd[b]	2.2	3.3	2.8	1.5	

[a] Mean signed deviation (in au^3) of calculated values relative to the experimental ones. [b] Root-mean-square deviation (in au^3) relative to the experimental values.

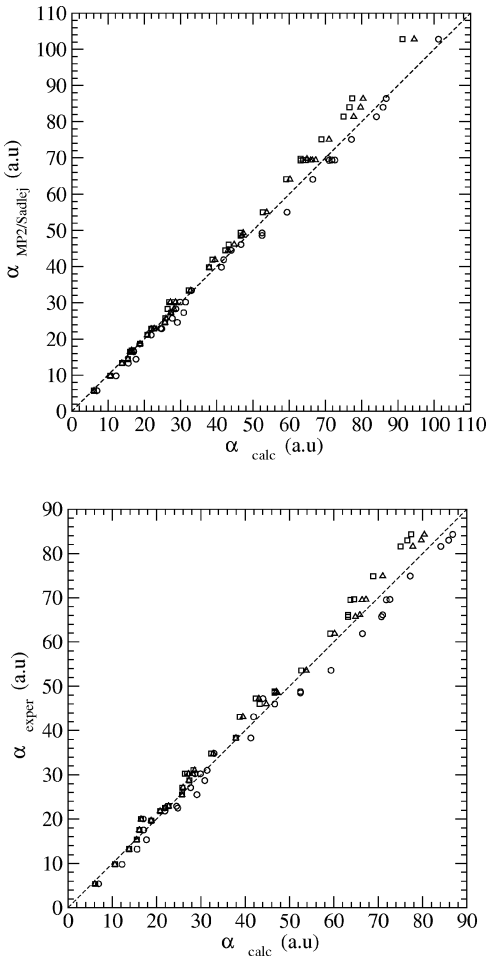

Figure 2. Comparison of the molecular polarizability (in au^3) determined at the MP2/Sadlej level (*top*) and experimentally (*bottom*) in front of the values obtained from distributed models A (triangle), B (square), and C (circle).

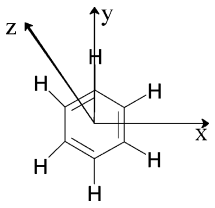

Figure 3. Orientations considered for the approach of a nonpolarizable point charge to benzene. The *x*-, *y*-, and *z*-axis corresponds to the approach along the axis passing (i) through the midpoint of the C−C bond, (ii) the C−H bond, and (iii) the center of the ring along the normal to the molecular plane.

to the center of the aromatic ring (*z*-direction). As noted in Figure 4, in all cases there is a rather promising agreement between the induction energies determined from the three distributed models and from MP2/Sadlej computations. This is particularly true in the range of distances corresponding to noncovalent interactions, especially for the approach of the nonpolarizable point charge along the *z*-axis, which corresponds to the cation-π interaction.

Figure 5 shows the variation in the magnitude of the total dipole moment induced in the benzene ring by the approach of the nonpolarizable positive point charge along the three different directions depicted in Figure 3. Keeping in mind the simplicity of the distributed models investigated here, which rely on isotropic atomic dipole polarizabilities, it is not surprising to find deviations between the induced dipole determined from MP2/Sadlej computations (carried out for the benzene in the presence and absence of the positive point charge) and from models A−C at those distances where the point charge penetrates the van der Waals region, where higher order polarization effects should be considered. At greater separations there is, however, qualitative agreement between the distance-dependent profiles obtained for the induced dipole moment determined from models A−C, which reproduce the trends witnessed at the quantum mechanical level.

Table 4 shows the polarization energies obtained variationally for a series of cation-π complexes constructed by placing a positive unit point charge at 2.5 Å along the normal axis passing through the center of the ring. The compounds include benzene and all its substituted derivatives, pyridine,

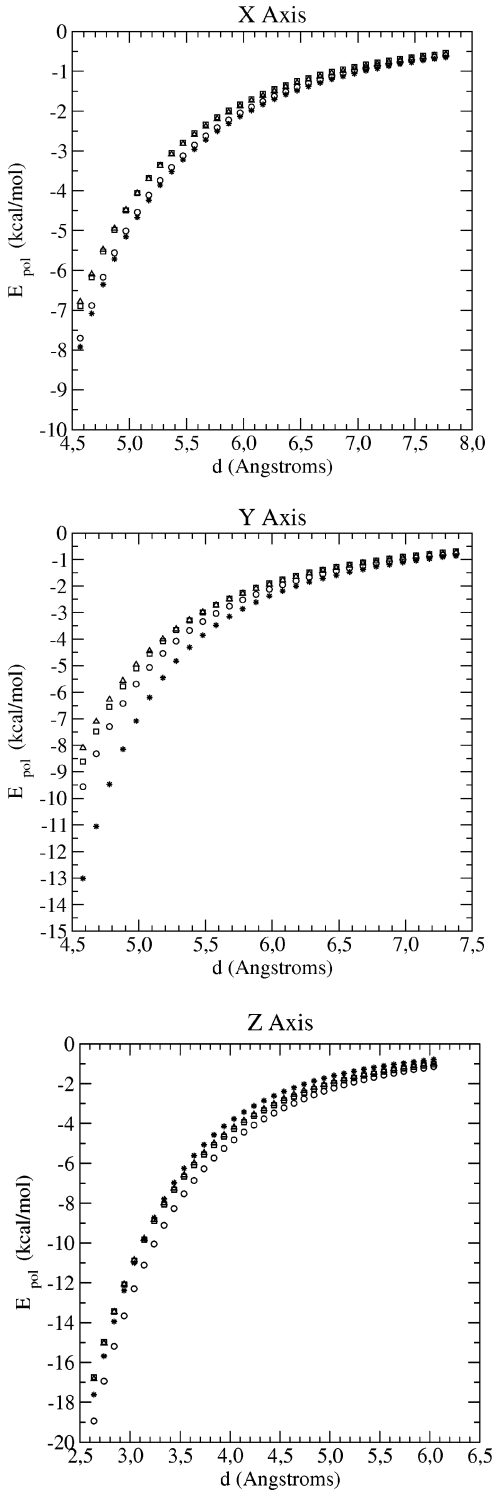

Figure 4. Induction energy profiles (in kcal/mol) for the approach of a positively charged particle to benzene determined from MP2/Sadlej calculations (black dots) and from distributed models A (triangle), B (square), and C (circle). Distances (in Å) are taken from the center of the benzene ring.

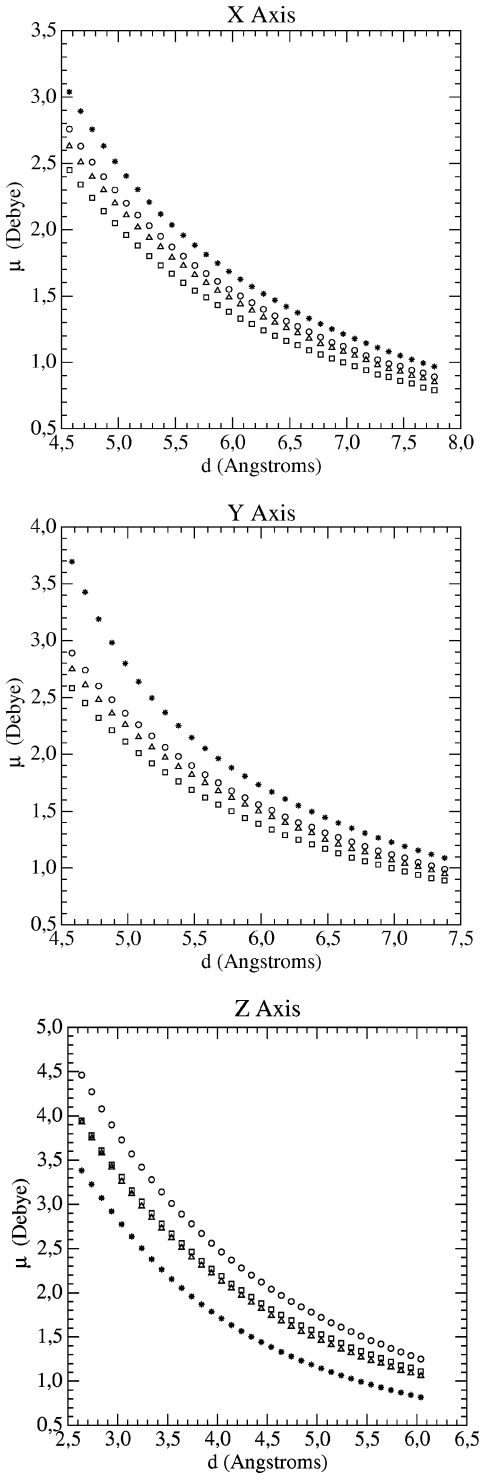

Figure 5. Induced dipole moment (in Debye) in the benzene molecule by a positively charged particle placed at different distances from the center of the ring determined from MP2/Sadlej calculations (black dots) and from distributed models A (triangle), B (square), and C (circle). Distances (in Å) are taken from the center of the benzene ring.

pyrrole, furan, imidazole, and indole (in the latter case, the positive charge was placed above the six-membered ring). For aniline and indole deviations between the MP2/Sadlej and classical induction energies of 4−5 kcal/mol are found, which suggests that at short intermolecular distances the simple models of distributed isotropic polarizabilities considered here might not be adequate to account properly for the induction effects felt by the polarizable sites in certain complexes. Nevertheless, in spite of the short distance separating the nonpolarizable point charge from the center of the ring, the polarization energies generally reproduce satisfactorily the MP2/Sadlej variational values, as the

Table 4. Induction Energies (in kcal/mol) Determined from Atomic Dipolar Polarizabilities Obtained from Models A−C and MP2/Sadlej Computations for Selected Cation-π Complexes

compound	A (eq 8, $\alpha>0$)	B (eq 9, $\alpha>0$)	C (eq 9, no restraint)	MP2/ Sadlej
benzene	−20.5	−20.3	−23.0	−21.4
indole	−19.4	−20.4	−21.2	−25.1
fluorobenzene	−19.4	−19.3	−21.9	−21.2
phenol	−19.5	−20.0	−22.3	−22.4
aniline	−19.8	−19.6	−21.9	−24.3
chlorobenzene	−20.5	−20.0	−22.6	−22.3
benzonitrile	−20.9	−20.8	−24.1	−22.2
1,4−difluorobenzene	−18.4	−18.5	−20.9	−21.0
1,3,5−trifluorobenzene	−18.3	−17.7	−19.9	−21.0
pyrrole	−19.9	−19.6	−22.2	−22.4
furan	−17.7	−17.8	−20.1	−20.5
imidazole	−15.9	−15.7	−17.7	−18.9
pyridine	−18.8	−18.7	−21.2	−19.8
msd[a]	2.6	2.6	0.3	
rmsd[b]	2.9	2.9	1.6	

[a] Mean signed deviation (in kcal/mol) of calculated values relative to the MP2/Sadlej ones. [b] Root-mean-square deviation (in kcal/mol) relative to the MP2/Sadlej induction energies.

deviations amount on average to 2.9 kcal/mol for models A and B and to 1.6 kcal/mol for model C.

As a final test to evaluate the goodness of the distributed models, we determined the induction energy for acetamide and pyridine in an aqueous environment. To this end, we selected five distinct configurations from Monte Carlo classical discrete simulations of those compounds solvated in an aqueous solution (TIP3P[91] water molecules). For each configuration, the induction energy created by the TIP3P water molecules on the solute was determined from MP2/Sadlej computations (see eq 1) and at the classical level using the atomic polarizabilities obtained from models A−C (eqs 8 and 9). In the two cases the water molecules were treated as an assembly of point particles located at the position of O and H atoms bearing the standard partial charges defined in the TIP3P model. The average induction energies determined by including the water molecules placed at 2.5, 4.5, 6.5, and 8.5 Å (around 6, 33, 77, and 150 waters, respectively) from the solute are shown in Figure 6. The results indicate that the induction energies estimated from models A−C reproduce satisfactorily the QM values, as noted in deviations between QM and classical polarization energies around 0.2 kcal/mol. In all cases the dependence of the induction energy on the distance of the water molecules from the solute is well captured by models A−C.

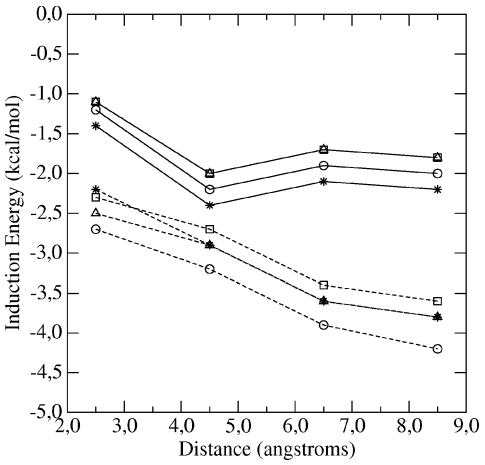

Figure 6. Induction energy (in kcal/mol) determined for acetamide (dashed) and pyridine (solid) in aqueous solution. The plot shows the average value of the induction energy determined from MP2/Sadlej calculations (star) and from distributed models A (triangle), B (square), and C (circle) for five distinct snapshots. Computations were performed by considering the solute at the QM level or classical levels and the water molecules (treated by using the TIP3P model) having any atom at a distance of 2.5, 4.5, 6.5, and 8.5 Å from any atom of the solute.

Conclusion

We have presented within the framework of the induced dipole model a computational strategy relying on the numerical fitting of atomic polarizabilities to induction energies determined from a perturbational scheme. Models of explicitly and implicitly interacting distributed polarizabilities have been considered. For a series of small, neutral organic compounds, our results indicate that the models reproduce rather nicely the molecular polarizability, as reflected in the RMSDs of about 3 au^3 for a series of compounds with a range of molecular polarizabilities close to 100 au^3. In addition, they predict in a satisfactory fashion the polarization energy determined variationally for a series of representative cation-π complexes, where induction effects have proven to contribute significantly to the stabilization energy of the complexes. They are also capable of reproducing the induction energy determined for acetamide and pyridine in aqueous environments.

For all intents and purposes, the present results suggest that the computational strategy outlined here can be a useful, effective tool to derive distributed models of atomic polarizabilities. Clearly, additional detailed studies are required to check the suitability of the models of both explicitly and implicitly interacting atomic polarizabilities in the framework of classical, discrete molecular simulations. At this point, it is worth noting that the distributed polarizability models considered here are rather simple, and they can be ameliorated in several ways, by including for instance charge-flow and quadrupole polarizabilities. In addition, the reliability of the distributed models must be supported by the accuracy in reproducing the induction energy determined at a high level of QM theory as well as in providing a correct description of anisotropy and nonadditivity features of induction forces for a variety of molecular complexes. Finally, the implementation of the distributed polarizabilities into a given force field must be accompanied by an extensive calibration of the different energy contributions and by appropriate corrections in order to maintain the subtle balance between the different energy contributions.[92] Even though the case examples tackled here were limited to models of isotropic atomic polarizabilities within the induced dipole

theory, extension of the computational strategy presented here to more elaborate models is expected to be rather straightforward.

Acknowledgment. This work was partially supported by grants from the Spanish Ministerio de Educación y Ciencia (grant CTQ2005-08797-C02-01/BQU). The Centre de Supercomputació de Catalunya (CESCA) is kindly acknowledged for computational facilities.

Supporting Information Available: Numbering of atoms in pyridine, pyrrole, furan, imidazole, and indole in Table 2 (Figure S1) and plots for the comparison of the atomic polarizabilities derived from models A−C (Figure S2). This material is available free of charge via the Internet at http://pubs.acs.org.

References

(1) Computer Simulation of Chemical and Biomolecular Systems. Beveridge, D. L., Jorgensen, W. L., Eds.; *Ann. N.Y. Acad. Sci.* **1986**, *482*, 1.

(2) Hehre, W. J.; Radom, L.; Schleyer, P. V. R.; Pople, J. A. *Ab Initio Molecular Orbital Theory*; Wiley-Interscience: New York, 1986.

(3) MacKerell, A. D., Jr.; Karplus, M. Importance of Attractive van der Waals Contribution in Empirical Energy Function Models for the Heat of Vaporization of Polar Liquids. *J. Phys. Chem*. **1991**, *95*, 10559.

(4) Pranata, J.; Wierschke, S. G.; Jorgensen, W. L. OPLS Potential Functions for Nucleotide Bases. Relative Association Constants of Hydrogen-Bonded Base Pairs in Chloroform. *J. Am. Chem. Soc*. **1991**, *113*, 2810.

(5) Carlson, H. A.; Nguyen, T. B.; Orozco, M.; Jorgensen, W. L. Accuracy of Free Energies of Hydration for Organic Molecules from 6-31G*-Derived Partial Charges. *J. Comput. Chem.* **1993**, *14*, 1240.

(6) Orozco, M.; Jorgensen, W. L.; Luque, F. J. Comparison of 6-31G*-Based MST/SCRF and FEP Evaluations of the Free Energies of Hydration for Small Neutral Molecules. *J. Comput. Chem.* **1993**, *14*, 1498.

(7) Bayly, C. I.; Cieplak, P.; Cornell, W.; Kollman, P. A. A Well-behaved Electrostatic Potential Based Method Using Charge Restraints for Deriving Atomic Charges: the RESP Model. *J. Phys. Chem*. **1993**, *97*, 10269.

(8) MacKerell, A. D., Jr., Wiórkiewicz-Kuczera, J.; Karplus, M. An All-Atom Empirical Energy Function for the Simulation of Nucleic Acids. *J. Am. Chem. Soc*. **1995**, *117*, 11946.

(9) Fox, T.; Kollman, P. A. Application of the RESP Methodology in the Parametrization of Organic Solvents. *J. Phys. Chem. B* **1998**, *102*, 8070.

(10) McDonald, N. A.; Jorgensen, W. L. Development of an All-Atom Force Field for Heterocycles. Properties of Liquid Pyrrole, Furan, Diazoles, and Oxazoles. *J. Phys. Chem. B* **1998**, *102*, 8049.

(11) Foloppe, N.; MacKerell, A. D., Jr. All-Atom Empirical Force Field for Nucleic Acids: I. Parameter Optimization Based on Small Molecule and Condensed Macromolecular Target Data. *J. Comput. Chem*. **2000**, *21*, 86.

(12) Price, M. L. P.; Ostrovsky, D.; Jorgensen, W. L. Gas-Phase and Liquid-State Properties of Esters, Nitriles, and Nitro Compounds with the OPLS-AA Force Field. *J. Comput. Chem*. **2001**, *22*, 1340.

(13) Chipot, C.; Ángyán, J. G.; Maigret, B.; Scheraga, H. A. Modeling Amino Acid Side XChains. 3. Influence of Intra- and Intermolecular Environment on Point Charges. *J. Phys. Chem.* **1993**, *97*, 9797.

(14) New, M. H.; Berne, B. J. Molecular Dynamics Calculation of the Effect of Solvent Polarizability on the Hydrophobic Interaction. *J. Am. Chem. Soc*. **1995**, *117*, 7172.

(15) Chipot, C.; Maigret, B.; Pearlman, D. A.; Kollman, P. A. Molecular Dynamics Potential of Mean Force Calculations: A Study of the Toluene-Ammonium π-Cation Interactions. *J. Am. Chem. Soc*. **1996**, *118*, 2998.

(16) Cieplak, P.; Caldwell, J.; Kollman, P. A. Molecular Mechanical Models for Organic and Biological Systems Going Beyond the Atom centered Two Body Additive Approximation: Aqueous Solution Free Energies of Methanol and N-Methyl Acetamide, Nucleic Acid Base, and Amide Hydrogen Bonding and Chloroform/Water Partition Coefficients of the Nucleic Acid Bases. *J. Comput. Chem*. **2001**, *22*, 1048.

(17) Allen, T. W.; Bastug, T.; Kuyucak, S.; Chung, S.-H. Gramicidin A Channel as a test Ground for Molecular Dynamics Force Fields. *Biophys. J*. **2003**, *84*, 2159.

(18) Grossfield, A.; Ren, P.; Ponder, J. W. Ion Solvation Thermodynamics from Simulation with a Polarizable Force Field. *J. Am. Chem. Soc*. **2003**, *125*, 15671.

(19) Patel, S.; Mackerell, A. D., Jr.; Brooks, C. L., III CHARMM Fluctuating Charge Force Field for Proteins: II Protein/Solvent Properties from Molecular Dynamics Simulations Using a Nonadditive Electrostatic Model. *J. Comput. Chem*. **2004**, *25*, 1504.

(20) Yan, T.; Burnham, C. J.; Del Pópolo, M. G.; Voth, G. A. Molecular Dynamics Simulation of Ionic Liquids: The Effect of Electronic Polarizability. *J. Phys. Chem. B* **2004**, *108*, 11877.

(21) Allen, T. W.; Andersen, O. S.; Roux, B. Energetics of Ion Conduction through the Gramicidin Channel. *Proc. Nat. Acad. Sci U.S.A.* **2004**, *101*, 117.

(22) Kim, B.; Young, T.; Harder, E.; Friesner, R. A.; Berne, B. J. Structure and Dynamics of the Solvation of Bovine Pancreatic Trypsin Inhibitor in Explicit Water: A Comparative Study of the Effects of Solvent and Protein Polarizability. *J. Phys. Chem. B* **2005**, *109*, 16529.

(23) Ishida, T. Polarizable Solute in Polarizable and Flexible Solvents: Simulation Study of Electron transfer Reaction Systems. *J. Phys. Chem. B* **2005**, *109*, 18558.

(24) Sakharov, D. V.; Lim, C. Zn Protein Simulations Including Charge Transfer and Local Polarization Effects. *J. Am. Chem. Soc*. **2005**, *127*, 4921.

(25) Guo, H.; Gresh, N.; Roques, B. P.; Salahub, D. R. Many-Body Effects in Systems of Peptide Hydrogen-Bonded Networks and Their Contributions to Ligand Binding: A Comparison of the Performances of DFT and Polarizable Molecular Mechanics. *J. Phys. Chem. B* **2000**, *104*, 9746.

(26) Tiraboschi, G.; Gresh, N.; Giessner-Prettre, C.; Pedersen, L. G.; Deerfield, D. W. Parallel ab Initio and Molecular Mechanics Investigation of Polyccordinated Zn(II) Complexes with Model Hard and Soft Ligands : Variations of Binding Energy and of its Components with Number and Charges of Ligands. *J. Comput. Chem.* **2000**, *21*, 1011.

(27) Gresh, N.; Piquemal, J.-P.; Krauss, M. Representation of Zn(II) Complexes in Polarizable Molecular Mechanics. Further Refinements of the Electrostatic and Short-Range Contributions. Comparisons with Parallel ab Initio Computations. *J. Comput. Chem.* **2005**, *26*, 1113.

(28) Gresh, N.; Sponer, J. Complexes of Pentahydrated Zn^{2+} with Guanine, Adenine, and the Guanine-Cytosine and Adenine-Thymine Base Pairs. Structures and Energies Characterized by Polarizable Molecular Mechanics and ab Initio Calculations. *J. Phys. Chem. B* **1999**, *103*, 11415.

(29) Rappé, A. K.; Goddard, W. A., III. Charge Equilibration for Molecular Dynamics Simulations. *J. Phys. Chem*. **1991**, *95*, 3358.

(30) Rick, S. W.; Stuart, S. J.; Berne, B. J. Dynamical Fluctuating Charge Force Fields: Application to Liquid Water. *J. Chem. Phys*. **1994**, *101*, 6141.

(31) Field, M. J. Hybrid Quantum Mechanical/Molecular Mechanical Fluctuating Charge Models for Condensed Phase Simulations. *Mol. Phys*. **1997**, *91*, 835.

(32) Banks, J. L.; Kaminsky, G. A.; Zhou, R.; Mainz, D. T.; Berne, B. J.; Friesner, R. A. *J. Chem. Phys*. **1999**, *110*, 741.

(33) Bret, C.; Field, M. J.; Hemmingsen, L. A Chemical Potential Equalization Model for Treating Polarization in Molecular Mechanical Force Fields. *Mol. Phys*. **2000**, *98*, 751.

(34) Applequist, J.; Carl, J. R.; Fung, K.-K. An Atom Dipole Interaction Model for Molecular Polarizability. Application to Polyatomic Molecules and Determination of Atom Polarizabilities. *J. Am. Chem. Soc*. **1972**, *94*, 2952.

(35) Warshel, A.; Levitt, M. Theoretical Studies of Enzymic Reactions: Dielectric, Electrostatic and Steric Stabilization of the Carbonium Ion in the Reaction of Lysozyme. *J. Mol. Biol*. **1976**, *103*, 227.

(36) Lybrand, T. P.; Kollman, P. A. Water-Water and Water-Ion Potential Functions Including Terms for Many Body Effects. *J. Chem. Phys*. **1985**, *83*, 2923.

(37) Caldwell, J.; Dang, L. X.; Kollman, P. A. Implementation of Nonadditive Intermolecular Potentials by Use of Molecular Dynamics: Development of a Water-Water Potential and Water-Ion Cluster Interactions. *J. Am. Chem. Soc*. **1990**, *112*, 9144.

(38) Voisin, C.; Cartier, A. Determination of Distributed Polarizabilities to be Used for Peptide Modeling. *J. Mol. Struct. (Theochem*) **1993**, *286*, 35.

(39) Meng, E. C.; Kollman, P. A. Molecular Dynamics Studies of the Properties of Water around Simple Organic Solutes. *J. Phys. Chem*. **1996**, *100*, 11460.

(40) Meng, E.; Caldwell, J. W.; Kollman, P. A. Investigating the Anomalous Solvation Free Energies of Amines with a Polarizable Potential. *J. Phys. Chem*. **1996**, *100*, 2367.

(41) Kamisnki, G. A.; Stern, H. A.; Berne, B. J.; Friesner, R. A.; Cao, Y. X.; Murphy, R. B.; Zhou, R.; Halgren, T. A. Development of a Polarizable Force Field for Proteins via ab Initio Quantum Chemistry: First Generation Model and Gas Phase Tests. *J. Comput. Chem*. **2002**, *23*, 1515.

(42) Ren, P.; Ponder, J. W. Consistent Treatment of Inter- and Intramolecular Polarization in Molecular Mechanics Calculations. *J. Comput. Chem*. **2002**, *23*, 1497.

(43) Borodin, O.; Smith, G. D. Development of Quantum Chemistry-Based Force Fields for Poly(ethylene oxide) with Many-Body Polarization Interactions. *J. Phys. Chem. B* **2003**, *107*, 6801.

(44) Kaminski, G. A.; Stern, H. A.; Berne, B. J.; Friesner, R. A. Development of an Accurate and Robust Polarizable Molecular Mechanics Force Field from ab Initio Quantum Chemistry. *J. Phys. Chem. A* **2004**, *108*, 621.

(45) Borodin, O.; Smith, G. D. Development of Many-Body Polarizable Force Fields for Li-Battery Components: 1. Ether, Alkane, and Carbonate Solvents. *J. Phys. Chem. B* **2006**, *110*, 6279.

(46) Cao, J.; Berne, B. J. Theory and Simulation of Polar and Nonpolar Polarizable Fluids. *J. Chem. Phys*. **1993**, *99*, 6998.

(47) Lamoureux, G.; Roux, B. Modeling Induced Polarization with Classical Drude Oscillators: Theory and Molecular Dynamics Simulation Algorithm. *J. Chem. Phys*. **2003**, *119*, 3025.

(48) Lamoureux, G.; MacKerell, A. D., Jr.; Roux, B. A Simple Polarizable Model of Water Based on Classical Drude Oscillators. *J. Chem. Phys*. **2003**, *119*, 5185.

(49) Winn, P. J.; Ferenczy, G. G.; Reynolds, C. A. Towards Improved Force Fields: III. Polarization thorugh Modified Atomic Charges. *J. Comput. Chem*. **1999**, *20*, 704.

(50) Ferenczy, G. G.; Reynolds, C. A. Molecular Polarization through Induced Atomic Charges. *J. Phys. Chem. A* **2001**, *105*, 11470.

(51) Curutchet, C.; Bofill, J. M.; Hernández, B.; Orozco, M.; Luque, F. J. Energy decomposition in Molecular Complexes: Implications for the Treatment of Polarization in Molecular Simulations. *J. Comput. Chem*. **2003**, *24*, 1263.

(52) Stern, H. A.; Kaminsky, G. A.; Banks, J. L.; Zhou, R.; Berne, B. J.; Friesner, R. A. Fluctuating Charge, Polarizable Dipole, and Combined Models: Parametrization from ab Initio Quantum Chemistry. *J. Phys. Chem. B* **1999**, *103*, 4730.

(53) Stern, H. A.; Rittner, F.; Berne, B. J.; Friesner, R. A. Combined Fluctuating Charge and Polarizable Dipole Models: Application to a Five-Site Water Potential Function. *J. Chem. Phys*. **2001**, *115*, 2237.

(54) Masia, M.; Probst, M.; Rey, R. On the Peformance of Molecular Polarization Methods. I. Water and Carbon Tetrachloride Close to a Point Charge. *J. Chem. Phys*. **2004**, *121*, 7362.

(55) Stone, A. J. Distributed Polarizabilities. *Mol. Phys.* **1985**, *56*, 1065.

(56) Le Sueur, C. R.; Stone, A. J. Localization Methods for Distributed Polarizabilities. *Mol. Phys.* **1994**, *83*, 293.

(57) Maaskant, W. J. A.; Oosterhof, L. J. Theory of Optical Rotatory Power. *Mol. Phys.* **1964**, *8*, 319.

(58) Stone, A. J. Distributed Multipole Analysis, or How to describe a Molecular Charge Distribution. *Chem. Phys. Lett.* **1981**, *83*, 233.

(59) Ángyán, J. G.; Jansen, G.; Loos, M.; Hättig, C.; Hess. B. A. Distributed Polarizabilities Using the Topological Theory of Atoms in Molecules. *Chem. Phys. Lett.* **1994**, *219*, 267.

(60) Bader, R. F. W. *Atoms in Molecules − A Quantum Theory*; Oxford University Press: London, 1990.

(61) Thole, B. T. Molecular Polarizabilities Calculated with a Modified Dipole Interaction. *Chem. Phys.* **1981**, *59*, 341.

(62) Applequist, J. Atom Charge Transfer in Molecular Polarizabilities. Application of the Olson-Sundberg Model to Aliphatic and Aromatic Hydrocarbons. *J. Phys. Chem*. **1993**, *97*, 6016.

(63) Miller, K. J. Additivity Methods in Molecular Polarizability. *J. Am. Chem. Soc*. **1990**, *112*, 8533.

(64) Stout, J. M.; Dykstra, C. E. Static Dipole Polarizabilities of Organic Molecules. Ab Initio Calculations and a Predictive Model. *J. Am. Chem. Soc*. **1995**, *117*, 5127.

(65) Zhou, T.; Dykstra, C. E. Additivity and Transferability of Atomic Contributions to Molecular second Dipole Hyperpolarizabilities. *J. Phys. Chem. A* **2000**, *104*, 2204.

(66) Bonaccorsi, R.; Petrongolo, C.; Scrocco, E.; Tomasi, J. Theoretical Investigations on the Solvation Process. *Theor. Chim. Acta* **1971**, *20*, 331.

(67) Momany, F. A. Determination of Partial Atomic Charges from ab Initio Molecular Electrostatic potentials. Application to Formamide, Methanol, and Formic Acid. *J. Phys. Chem.* **1978**, *82*, 592.

(68) Cox, S. R.; Williams, D. E. Representation of the Molecular Electrostatic potential by a Net Atomic Charge Model. *J. Comput. Chem.* **1981**, *2*, 304.

(69) Nakagawa, S.; Kosugi, N. Polarized One-Electron Potentials Fitted by Multicenter Polarizabilities and Hyperpolarizabilities. Ab Initio SCF-CI Calculation of Water. *Chem. Phys. Lett.* **1993**, *210*, 180.

(70) Alkorta, I.; Bachs, M.; Perez, J. J. The Induced Polarization of the Water Molecule. *Chem. Phys. Lett.* **1994**, *224*, 160.

(71) Celebi, N.; Ángyán, J. G.; Dehez, F.; Millot, C.; Chipot, C. Distributed Polarizabilities Derived from Induction Energies: A Finite Perturbation Approach. *J. Chem. Phys.* **2000**, *112*, 2709.

(72) Dehez, F.; Soetens, J. C.; Chipot, C.; Ángyán, J. G.; Millot, C. Determination of Distributed Poalrizabilities from a Statistical Analysis of Induction Energies. *J. Phys. Chem. A* **2000**, *104*, 1293.

(73) Luque, F. J.; Orozco, M. Polarization Effects in Generalized Molecular Interaction Potential: New Hamiltonian for Reactivity Studies and Mixed QM/MM Calculations. *J. Comput. Chem.* **1998**, *19*, 866.

(74) Cubero, E.; Luque, F. J.; Orozco, M. Is Polarization Important in Cation-Pi Interactions? *Proc. Natl. Acad. Sci. U.S.A.* **1998**, *95*, 5976.

(75) Chipot, C.; Dehez, F.; Ángyán, J.; Millot, C.; Orozco, M.; Luque, F. J. Alternative Approaches for the calculations of Induction Energies: Characterization, Effectiveness, and Pitfalls. *J. Phys. Chem. A* **2001**, *105*, 11505.

(76) Dehez, F.; Chipot, C.; Millot, C.; Ángyán, J. G. *Chem. Phys. Lett.* **2001**, *338*, 180.

(77) Francl, M. M. Polarization Corrections to Electrostatic Potentials. *J. Phys. Chem*. **1985**, *89*, 428.

(78) Chipot, C.; Luque, F. J. Fast Evaluation of Induction Energies: A Second-Order Perturbation Theory Approach. *Chem. Phys. Lett.* **2000**, *332*, 190.

(79) Chipot, C.; Ángyán, J. G. Continuing Challenges in the Parametrization of Intermolecular Force Fields. Towards and Accurate Description of Electrostatic and Induction Terms. *New. J. Chem.* **2005**, *29*, 411.

(80) Voisin, C.; Cartier, C.; Rivail, J. L. Computation of Accurate Electronic Molecular Polarizabilities. *J. Phys. Chem*. **1992**, *96*, 7966.

(81) Liu, S. Y.; Dykstra, C. E. Multipole Polarizabilities and Hyperpolarizabilities of AHn and A2Hn Molecules from Derivative Hartree-Fock Theory. *J. Phys. Chem*. **1987**, *91*, 1749.

(82) Spackman, M. A. A Simple Quantitative Model of Hydrogen Bonding. *J. Chem. Phys*. **1986**, *85*, 6587.

(83) Sadlej, A. J. Medium-Size Polarized Basis Sets for High-Level Correlated Calculations of Molecular Electric Properties. *Collect. Czech. Chem. Commun*. **1988**, *53*, 1995.

(84) Frisch, M. J.; Trucks, G. W.; Schlegel, H. B.; Scuseria, G. E.; Robb, M. A.; Cheeseman, J. R.; Montgomery, J. A., Jr.; Vreven, T.; Kudin, K. N.; Burant, J. C.; Millam, J. M.; Iyengar, S. S.; Tomasi, J.; Barone, V.; Mennucci, B.; Cossi, M.; Scalmani, G.; Rega, N.; Petersson, G. A.; Nakatsuji, H.; Hada, M.; Ehara, M.; Toyota, K.; Fukuda, R.; Hasegawa, J.; Ishida, M.; Nakajima, T.; Honda, Y.; Kitao, O.; Nakai, H.; Klene, M.; Li, X.; Knox, J. E.; Hratchian, H. P.; Cross, J. B.; Adamo, C.; Jaramillo, J.; Gomperts, R.; Stratmann, R. E.; Yazyev, O.; Austin, A. J.; Cammi, R.; Pomelli, C.; Ochterski, J. W.; Ayala, P. Y.; Morokuma, K.; Voth, G. A.; Salvador, P.; Dannenberg, J. J.; Zakrzewski, V. G.; Dapprich, S.; Daniels, A. D.; Strain, M. C.; Farkas, O.; Malick, D. K.; Rabuck, A. D.; Raghavachari, K.; D. K. Malick, Foresman, J. B.; Ortiz, J. V.; Cui, Q.; Baboul, A. G.; Clifford, S.; Cioslowski, J.; Stefanov, B. B.; Liu, G.; Liashenko, A.; Piskorz, P.; Komaromi, I.; Martin, R. L.; Fox, D. J.; Keith, T.; Al-Laham, M. A.; Peng, C. Y.; Nanayakkara, A.; Challacombe, M.; Gill, P. M. W.; Johnson, B.; Chen, W.; Wong, M. W.; Gonzalez, C.; Pople, J. A. *Gaussian03*, *Revision B.04*; Gaussian, Inc.: Pittsburgh, PA, 2003.

(85) Curutchet, C.; Alhambra, C.; Orozco, M.; Luque, F. J. *MOPETE*; University of Barcelona: Barcelona, 2003.

(86) Ángyán, J. G.; Chipot, C.; Dehez, F.; Hättig, C.; Jansen, G.; Millot, C. OPEP: A Tool for the Optimal Partitioning of Electric Properties. *J. Comput. Chem.* **2003**, *24*, 997.

(87) Ángyán, J. G.; Chipot, C.; Dehez, F.; Hättig, C.; Jansen, G.; Millot, C. *OPEP*; Université Henri Poincaré: Nancy, 2002.

(88) Bondi, A. van der Waals Volumes and Radii. *J. Phys. Chem*. **1964**, *68*, 441.

(89) Soteras, I.; Orozco, M.; Luque, F. J. *FITPOL*; University of Barcelona: Barcelona, 2006.

(90) Atomic and Molecular Polarizabilities. In *CRC Handbook of Chemistry and Physics*, Internet Version 2007 (87th ed.); Lide, D. R., Ed.; Taylor and Francis: Boca Raton, FL.

(91) Jorgensen, W. L.; Chandrasekhar, J.; Madura, J. D.; Impey, R. W.; Klein, M. L. Comparison of Simple Potential Functions for Simulating Liquid Water. *J. Chem. Phys.* **1983**, *79*, 926.

(92) Dehez, F.; Angyán, J. G.; Soteras Gutiérrez, I.; Luque, F. J.; Shulten, K.; Chipot, C. Modeling Induction Phenomena in Intermolecular Interactions with an ab Initio Force Field. *J. Chem. Theor. Comput*. **2007**, *3*, 1914−1926.

CT7001122